ACS OMEGA

http://pubs.acs.org/journal/acsodf

Article

Amine-Functionalized Nanoporous Silica Monoliths for Heterogeneous Catalysis of the Knoevenagel Condensation in Flow

Kevin Turke, Rafael Meinusch, Pascal Cop, Eric Prates da Costa, Raoul D. Brand, Anja Henss, Peter R. Schreiner, and Bernd M. Smarsly*

Cite This: *ACS Omega* 2021, 6, 425−437

Read Online

ACCESS | Metrics & More | Article Recommendations | Supporting Information

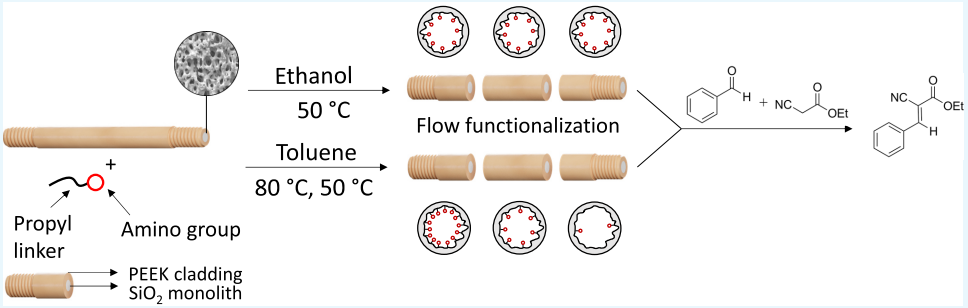

ABSTRACT: Porous carrier materials functionalized with organocatalysts offer substantial advantages compared to homogeneous catalysts, e.g., easy separation of the catalyst, scalability, and an improved implementation in continuous operations. Here, we report the immobilization of (3-aminopropyl)trimethoxysilane (APTMS) onto self-prepared silica monoliths and its application as a heterogeneous catalyst in the Knoevenagel condensation between cyano ethylacetate and various aromatic aldehydes under continuous-flow conditions. The meso-macroporous silica monoliths (6−7 cm in length) were optimized to be used in flow taking advantage of their hierarchical meso- and macroporosity. The monoliths were cladded with a poly(ether ether ketone) (PEEK) tube by a refined procedure to guarantee tight connection between the carrier material and PEEK. Functionalization of the bare silica monoliths consisting of APTMS can be efficiently performed in flow in ethanol and toluene. While a large grafting gradient is obtained for toluene, the grafting in ethanol proceeds homogenously throughout the monolith, as evidenced by elemental analysis and time-of-flight secondary ion mass spectrometry (ToF-SIMS). The silica monoliths exhibit high conversion up to 95% with concurrent low back pressures, which is of importance in flow catalysis. By connecting two monoliths, high conversions can be maintained for several flow rates. Two types of monoliths were synthesized, possessing different mesopore sizes. The monolith bearing the larger mesopore size showed an enhanced turnover frequency (TOF), while the monolith with the smaller mesopores allowed for larger quantities of the product to be synthesized, due to the higher surface area. A long-term stability test showed that the functionalized monoliths were still active after 66 h of continuous usage, while the overall yield decreased over time.

1. INTRODUCTION

The functionalization of porous inorganic materials with organocatalysts offers improved reusability of the catalysts and an easy workup and purification, since no separation of the catalyst from the reaction mixture is needed. Additionally, these heterogeneous catalysts can easily be used as continuous-flow reactors.[1−4] Implementation in sophisticated reactor designs, e.g., continuous-flow multistep reactions, offers a great opportunity toward green chemistry and sustainable chemical synthesis.[5] A widely used carrier material for organocatalysts is porous silica.[6−10] Owing to its large surface area, often spanning several hundred square meters, large quantities of catalyst can be immobilized onto the surface. In addition, its mechanical and chemical stability along with the absence of swelling in many organic solvents makes it particularly suitable to be used in flow catalysis. Commonly, bed reactors containing packed SiO_2 or polymer particles are used for continuous operations.[11−13] A prominent example is the synthesis of the anti-inflammatory drug rolipram by Tsubogo et al.[14] By connecting several packed-bed reactors with different catalysts, the final product can be obtained in good yield and high enantiomeric excess. However, because of the random packing of the sometimes simply crushed particles detrimental fluid mechanics ensue and the formation of stagnation zones and high back pressures might occur.

Received: October 5, 2020
Accepted: December 7, 2020
Published: December 21, 2020

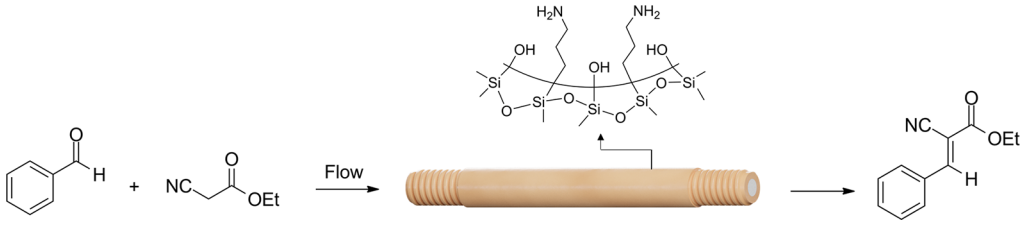

Figure 1. Schematic depiction of a cladded and functionalized monolithic silica reactor and its application as a heterogeneous catalyst for the continuous-flow Knoevenagel condensation.

Additionally, mechanical attrition after their long-term use hinders the reusability of these materials.

Meso-macroporous silica monoliths represent a potential alternative to packed SiO_2 particles.[15−17] This special type of porous SiO_2 consists of a continuous network of macropores with mesopores distributed inside the silica skeleton. The macroporous network allows for fast transport of the reactants to the mesopores. Owing to their large surface area, introduced by the mesopores, they can be easily functionalized with large amounts of catalyst. The synthesis of silica monoliths with bimodal pore structures was optimized by Nakanishi et al.[18] By this so-called Nakanishi process, a wide range of meso- and macropore sizes can be independently tailored. Based on this synthesis, silica monoliths have been previously functionalized with organocatalysts and enzymes and were used in batch and flow catalysis.[19−22] The first functionalized silica monoliths to be used in flow organocatalysis were reported by El Kadib et al.[23] Here, monoliths were functionalized in flow with either amine or sulfonic acid groups.

Both materials offered high yield for the Knoevenagel condensation (with an amine as the catalyst, exemplarily depicted with a cladded monolith in Figure 1) and the transesterification of triacetine (with sulfonic acid). In addition, Haas et al. demonstrated that functionalized silica monoliths can readily be used to determine intrinsic reaction kinetics.[24] However, in spite of the potential of such meso-macroporous SiO_2 monoliths, the number of studies addressing the immobilization of organocatalysts is small, partially because of the complex synthesis of the material itself and the functionalization.

Functionalization of silica monoliths and silica materials is often accomplished by a grafting procedure.[25,26] Therefore, a suitable catalyst precursor, e.g., a silane or a silyl chloride carrying the catalytic group, can be anchored on the silica surface via condensation reactions with the free silanol groups under the formation of relatively stable siloxane bonds. Many precursors are commercially available and readily used in research and industry. However, prior to being used as a microreactor, the monoliths must be surrounded by a suitable housing material to connect and adapt them to a flow system, which constitutes a major challenge in the use of such monoliths. For that purpose, shrinkable poly(tetrafluoroethylene) (PTFE) or glass tubes are used.[27,28] Additionally, cladding with stainless steel is feasible.[29,30] A further challenge lies with the necessity of applying a certain sequence in the synthesis and construction of the overall reactor. Since the relatively high temperatures required for many cladding procedures modify or even degrade the organocatalysts, functionalization prior to cladding is unfeasible.

To overcome this problem, grafting under continuous-flow conditions is an alternative route for the immobilization of organocatalysts, which is pursued in the present study. In this case, a solution containing the grafting precursor is continuously pumped through the monolith. After the reaction, residual amounts of the precursor are washed out of the microreactor. Yet, grafting under continuous-flow conditions might potentially result in an inhomogeneous distribution of the immobilized catalyst, in particular, in the form of radial or longitudinal gradients. An inhomogeneously distributed catalyst can possibly affect the catalytic performance as it causes the catalyst motifs to be too close to each other, which might decrease the overall efficiency, for instance, by clogging the mesopores. Thus, knowledge of the catalyst distribution throughout the whole microreactor is a key parameter to ensure efficient reaction control. To the best of our knowledge, the spatial homogeneity in the functionalization with an organocatalyst immobilized under continuous-flow conditions on silica materials has not yet been discussed in detail, while we regard it as quite significant for the usage of such material systems in catalysis. To address this problem, we have functionalized silica monoliths in flow with (3-aminopropyl)trimethoxysilane (APTMS) to incorporate an aminopropyl group into the material as a catalytic motif. APTMS is a commonly used precursor for introducing basic amine groups on different carrier materials.[31,32] Based on a thorough characterization of these materials, several parameters affecting catalytic performance were studied to elucidate their relevance for optimizing the catalytic properties. Thus, we have varied the mesopore size to study a possible pore-size effect on the catalytic performance of our reactors. It has been demonstrated for many reactions that the conversion rate is highly dependent on the ratio of the pore diameter and the reactant molecules as the diffusion rate decreases for smaller pore diameters.[33,34] The meso-macroporous SiO_2 monoliths are ideal to address this parameter, as the mesopore dimension can be varied independently of the macropore size, thus allowing for the disentanglement of the mesopore size effect on catalytic properties.

As a second parameter, we used different solvents, as previous studies suggested an impact on the grafting progress.[35,36] Namely, a protic solvent can induce a homogeneous distribution inside the reaction mixture by forming hydrogen bonds between the solvent and the free amine groups of APTMS.[37] In contrast, a solvent that is not capable of forming hydrogen bonds may lead to an inhomogeneous distribution of the precursor. For that purpose, we have chosen ethanol and toluene as solvents. Additionally, the functionalization for both solvents was conducted at different temperatures to study the influence of elevated temperatures on the grafting homogeneity. To elucidate the distribution of the catalyst within the monoliths, for each cladded monolith, the front and the end part were intensively characterized by argon physisorption and elemental

https://dx.doi.org/10.1021/acsomega.0c04857
ACS Omega 2021, 6, 425−437

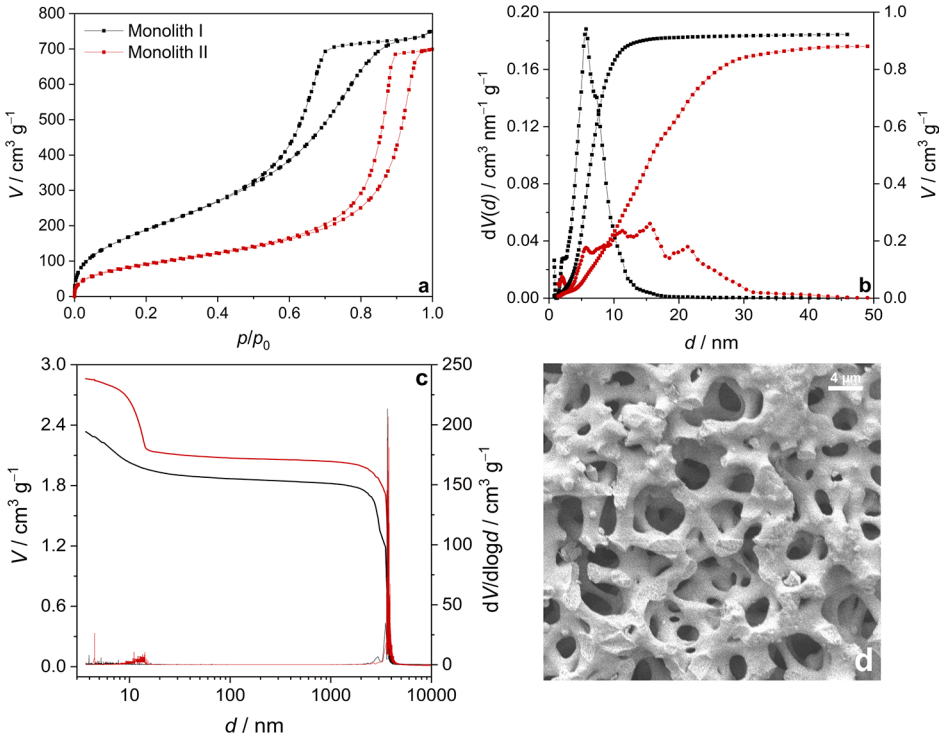

Figure 2. Argon physisorption isotherms (a) and differential and cumulative pore volumes (b) of the two types of monoliths used in this study. Because of the higher temperature during hydrothermal treatment, monolith II exhibits a much broader pore-size distribution. Cumulative and differential pore sizes for both monoliths obtained by mercury intrusion porosimetry (c). Scanning electron microscopy (SEM) micrograph of one synthesized silica monolith gelled at 22 °C (d).

analysis measurements to study the grafting homogeneity, complemented by time-of-flight secondary ion mass spectrometry (ToF-SIMS), providing a radial distribution profile. The present study is also intended to show the potential of ToF-SIMS for unraveling the spatial distribution of functional moieties in such porous monoliths, which is difficult to obtain by other techniques.

The housing for the monoliths represents a challenge in itself, as the cladding must ensure a tight surrounding without any crack with respect to both, the functionalization and the catalysis. For our monoliths, we adapted and refined the process of cladding from Chamieh et al. by combining a heat-shrinkable PTFE tube and a poly(ether ether ketone) (PEEK) tube with a defined inner diameter.[38] Owing to its mechanical and chemical stability, PEEK is suitable to be used as a cladding material for continuous-flow catalysis. To enable reproducibility of the cladding procedure, we developed a modified process, which is described in detail in the experimental part. In short, monolithic silica rods are placed inside PEEK tubes, which themselves are surrounded by PTFE tubes. Upon heating, PEEK becomes viscous so that it can be pressed radially onto the silica rod, induced by the shrinking PTFE tube. The resulting tight connection between the PEEK tube and the silica monolith is an important parameter for flow catalysis to ensure that the reaction mixture flows through the silica network.

To establish such functionalized monoliths to be used in heterogeneous-flow catalysis, their performance was studied in the Knoevenagel condensation, a widely used organic reaction to form carbon−carbon double bonds.[39,40] The aminopropyl entity was used as the catalytic motif because it can be easily attached to the pore surface and does hardly undergo degradation reactions, when compared to more complex organocatalysts. Also, the Knoevenagel condensation, catalyzed by this motif, is sufficiently simple to study the aforementioned fundamental parameters. Therefore, we have varied several reaction parameters, especially the flow rate, the catalyst loading, and the distribution of the catalyst inside the reactor, to investigate the influence of each parameter on product formation. Until now, only the reaction of benzaldehyde and cyano ethylacetate has been discussed in the literature for functionalized silica monoliths. While these two reactants are suitable for an overall catalysis test, the investigation of different reactants is needed to study the practical application of these reactors. Accordingly, a product screening as well as a long-term stability test was conducted to enhance the scope of the functionalized monoliths as reactors in continuous-flow organocatalysis.

2. RESULTS AND DISCUSSION

2.1. Characterization of the Unfunctionalized Silica Monoliths. Two silica monoliths with different mesopore diameters, but identical macropore dimension, were synthesized by a modified Nakanishi process.[18,41] We used poly(ethylene glycol) (PEG) 10k and acetic acid to ensure fast hydrolysis and gelation of the silane precursor. Variation of the mesopore diameter was conducted by changing the hydrothermal treatment conditions for both monoliths (see the Section 4). Both samples were studied by argon physisorption measurements (Figure 2a,b) at 87 K. Compared to commonly used nitrogen, argon does not exhibit a quadrupole moment, which makes a comprehensive analysis difficult because the use of nitrogen overestimates the specific surface area of silica by about 25%.[42,43]

https://dx.doi.org/10.1021/acsomega.0c04857
ACS Omega 2021, 6, 425−437

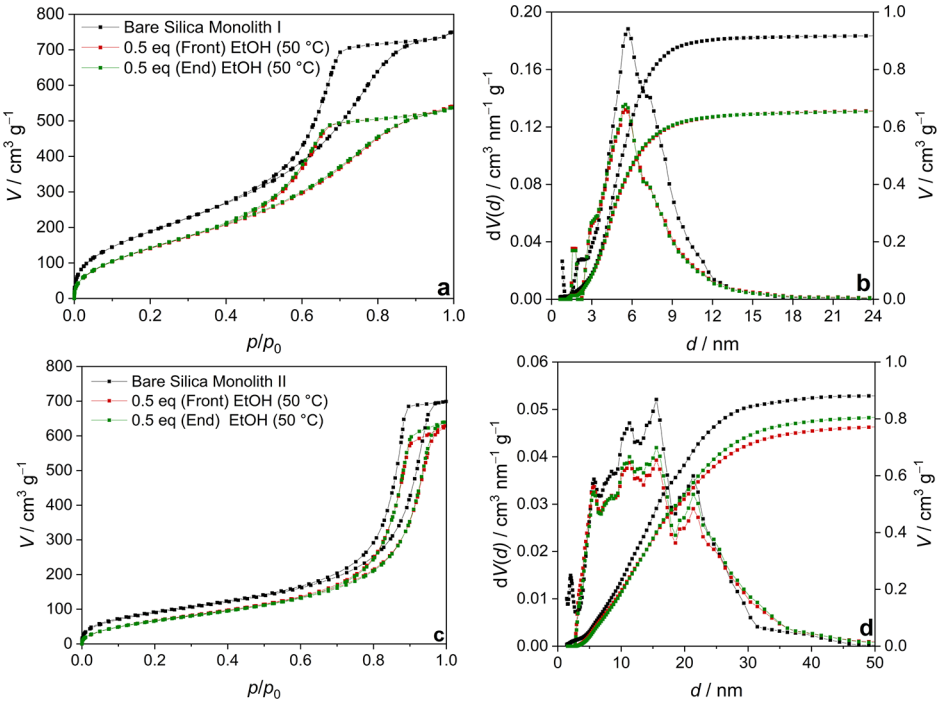

Figure 3. Argon physisorption isotherms of functionalized monolith I (a) and monolith II (c). Grafting was performed in ethanol at 50 °C using 0.5 equiv of APTMS. The coinciding pore-size distributions (nonlocal density functional theory (NLDFT), ads, cyl. pore model) obtained from the front and the end of both monolith I (b) and monolith II (d) reveal a homogeneous grafting along the monoliths.

Both samples feature a type IV(a) isotherm, which is typically observed for mesoporous materials.[44] A detailed physisorption study of the unfunctionalized silica monoliths is beyond the scope of this work and will be discussed in a separate publication. Monolith I offers a specific surface area of 659 $m^2\ g^{-1}$ and a mean mesopore size of 6.8 nm (Table S1). Because of the higher temperature during hydrothermal treatment, monolith II exhibits a smaller specific surface area (303 $m^2\ g^{-1}$) but at the same time a larger mean mesopore size of 15.9 nm. Additionally, its pore-size distribution broadens significantly due to the continuous solvation and precipitation of silica during hydrothermal treatment. The mesopore volumes on the other hand are almost identical for both samples (0.9 mL g^{-1}). The gelation temperature was kept at 22 °C for both monoliths to ensure a comparable macropore size of 3.5−4.0 μm, as determined by mercury intrusion porosimetry and scanning electron microscopy (Figure 2c,d). Identical macropore sizes are important for this study to ensure comparable fluid mechanics and back pressures.

2.2. Grafting of APTMS in Ethanol. Continuous-flow functionalization experiments were conducted in ethanol at 50 °C. APTMS was dissolved in dry ethanol and pumped through the monoliths for 18 h at a flow rate of 0.2 mL min^{-1}. No catalyst (acid or base) for spurring the sol−gel reaction was added to avoid self-condensation of the silane in solution. After flushing the monolith with ethanol and subsequent drying, the front and the end of each functionalized monolith were characterized independently by argon physisorption and elemental analysis. Since the mass of the monolith increases upon grafting, the corresponding physisorption data must be normalized to the same silica content (eq 1). Otherwise, porosity data of the functionalized samples might be significantly underestimated if no normalization is conducted.

$$m_{\text{normalized}} = m_{\text{initial}} \cdot (1 - (X \cdot M_{\text{catalyst}})) \quad (1)$$

Here, m_{initial} is the mass of the noncorrected sample, X is the catalyst loading of the material, and M_{catalyst} is the molar mass of the immobilized aminopropyl catalyst.

For several samples, we observed a higher carbon-to-nitrogen ratio (C/N = 4−5) than is to be expected for a fully hydroxylated aminopropyl group (C/N = 3). Accordingly, we used the molar mass of a grafted aminopropyl group, which still contains on average one nonhydrolyzed methoxy group (M_{catalyst} = 0.117 g $mmol^{-1}$) to match the experimental C/N values appropriately. The influence of normalization on the physisorption data is illustrated in Figure S5. Normalization to the same silica content results in a shift to larger adsorbed volumes for both isotherms. Additionally, the gap between both isotherms decreases and thus reflects the small grafting gradient that is present in this sample (0.2 equiv of APTMS; see Figure S5). Note that in most previous publications on functionalized SiO_2 such normalization of the porosity data is absent. However, we believe that the normalization to the SiO_2 mass, and not to the mass of SiO_2 plus the catalyst, is more appropriate to see the reduction in mesoporosity due to the functionalization. The amount of APTMS used for grafting refers to estimated 4.6 silanol groups per nm^2 on the silica surface.[45] For example, using 1.0 equiv of APTMS, the solution contains one APTMS molecule for each silanol group, which equals to an excessive amount of APTMS. For both monoliths, argon physisorption indicates a homogeneous grafting throughout the whole monolith for the grafting of 0.5 equiv of APTMS (Figure 3). The isotherms as well as the corresponding pore-size distributions of the front and the end coincide well for both monoliths. The pore volumes of the functionalized monoliths I and II significantly decrease between 5−12 and 5−25 nm, respectively, which is due to the grafting of the aminopropyl catalyst. Furthermore, the grafting homogeneity is independent of the amount of APTMS (Table S2). Catalyst loadings calculated from the nitrogen

https://dx.doi.org/10.1021/acsomega.0c04857
ACS Omega 2021, 6, 425−437

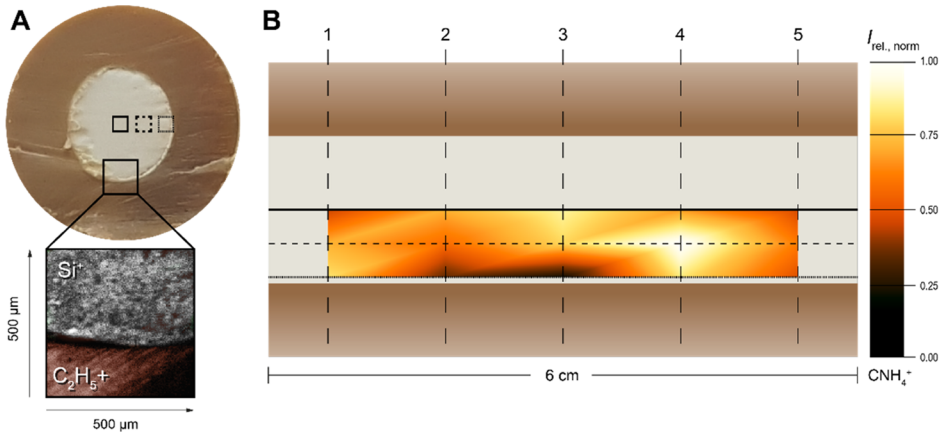

Figure 4. (A) Photograph of the PEEK-cladded silica monolith (length: 6 cm) with Si^+ and $C_2H_5^+$ ion images resembling the SiO_2 matrix and PEEK, respectively. (B) ToF-SIMS analysis: local ion intensity of CNH_4^+ in the silica monolith at the areas highlighted as solid, dashed, and dotted lines in (A) dependent on the length of the monolith. Since only the cutting areas were investigated, the relative ion counts were extrapolated by a color gradient for the intermediate space.

weight percentage increase for higher equivalents of APTMS. For 0.2 equiv of APTMS, only a minor grafting gradient can be obtained with an averaged catalyst loading of 0.90 mmol g^{-1}. By increasing the equivalents to 0.5 and 1.0 equiv, the loadings can be increased to 1.54 and 1.96 mmol g^{-1}, respectively. The Brunauer–Emmett–Teller (BET) surface areas obtained from the argon physisorption measurements decrease from 600 m^2 g^{-1} (0.2 equiv) to 510 m^2 g^{-1} (0.5 equiv). However, the surface area only slightly changes by increasing the amount of APTMS up to 1.0 equiv, which agrees well with assuming a monolayer type of functionalization. For 0.5 equiv, already a large surface concentration of the catalyst of about 2.3 μmol m^{-2} is obtained. Owing to its smaller surface area, the catalyst loading is smaller for monolith II compared to monolith I. Nevertheless, the functionalized monolith II still features the absence of a grafting gradient. Using 0.5 equiv of APTMS, 0.82 mmol g^{-1} of the catalyst can be grafted onto the material, which refers to a surface concentration of 2.7 μmol m^{-2}. Lowering the amount to 0.2 equiv results in a decreased catalyst loading (0.44 mmol g^{-1}). On the other hand, increasing the amount of APTMS to 1.0 equiv only slightly affects the catalyst loading (0.75 mmol g^{-1}). In summary, for continuous-flow functionalization, ethanol seems to be a suitable solvent to achieve a homogeneous functionalization along the monolith, which was addressed by Asefa et al.[36] who argued that APTMS forms hydrogen bonds with ethanol. Owing to the hydrogen bonds, APTMS becomes homogeneously distributed in solution, which in turn results in a homogeneous longitudinal grafting along the material. Additionally, one monolith was cut in half and immersed in a ninhydrin solution (Figure S21). Upon reacting with ninhydrin, the monolith showed an intense purple color, providing further evidence that the functionalization occurred inside the whole monolith.

In addition, ToF-SIMS measurements were performed to study the homogeneity of the grafting inside one functionalized monolith (0.5 equiv of APTMS in ethanol at 50 °C). As sputtering processes would lead to the destruction of the catalyst, the monolith was cut into five equal pieces and investigated each at three different spots (Figure 4A). Here, Si^+, $C_2H_5^+$, and CNH_4^+ (e.g., $H_2C{=}NH_2^+$) were chosen as representative ion species for the silica matrix, the PEEK cladding material, and the aminopropyl group, respectively. The latter is used to detect the progress of the functionalization within the length and depth of the monolith and is only detectable in the functionalized samples. By integrating the area of the CNH_4^+-ion signal, the values were normalized on the ion dose (10^{12} ions cm^{-2}) to calculate the relative intensity as a descriptor for the amount of functional groups on the silica matrix (Figure 4B). ToF-SIMS data show distinctive functionalization of the monolith, both radially and longitudinally; hence, ToF-SIMS allows for detecting and localizing the catalyst. However, in the middle part near the edge of the monolith (position 3 in Figure 4B), the signal intensity referring to the aminopropyl group significantly decreases. The lower grafting density right at this region might be induced by an insufficient connection between the silica framework and PEEK for this functionalized monolith. Accordingly, the grafting solution is likely to flow past the silica framework at this point as the hindrance is much lower. This is in accordance with the higher grafting density at point 4. Here, the connection between silica and PEEK is tight enough to force the grafting solution to flow through the silica framework again, resulting in an increased grafting density at point 4. It must be mentioned that the ToF-SIMS measurements are supposed to be a proof of concept for the investigation of functionalized silica monoliths with respect to the spatial distribution of the catalyst, especially for small catalytic groups like the aminopropyl group. Further experiments, e.g., the ToF-SIMS analysis of the other half of the functionalized monolith, are crucial to study the radial catalyst distribution in detail.

2.3. Grafting of APTMS in Toluene. In addition to ethanol, we studied the grafting behavior of APTMS in toluene. Although being mainly used under reflux conditions, we have lowered the reaction temperature to 80 and 50 °C because handling toluene near its boiling point was not feasible with our reaction setup. Compared to the grafting procedure in ethanol, a distinctive grafting gradient can be observed with toluene. This effect is independent of the temperature and the amount of APTMS used for grafting (for further details, please refer to the Supporting Information (SI)). Notably, the largest grafting gradient results from the grafting of 0.2 equiv of APTMS in toluene at 80 °C. Here, exclusively the front of the monolith was functionalized (1.83 mmol g^{-1}), while the end part was almost devoid of the aminopropyl group as the

https://dx.doi.org/10.1021/acsomega.0c04857
ACS Omega 2021, 6, 425−437

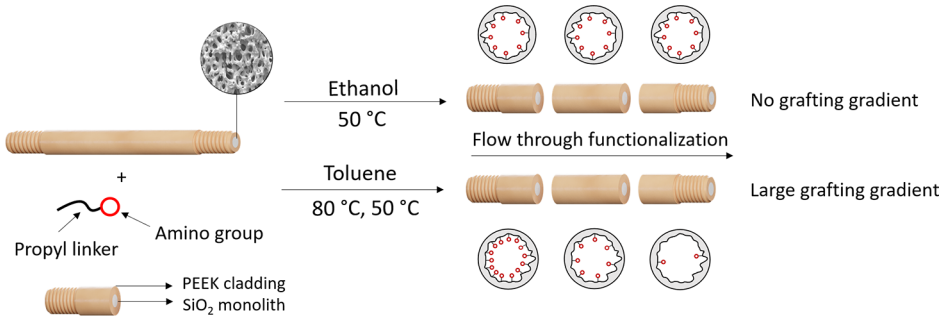

Figure 5. Schematic depiction of the longitudinal grafting behavior of APTMS in ethanol and toluene. Grafting in ethanol leads to a homogeneous catalyst loading throughout the monolith. However, grafting in toluene results in a strong grafting gradient between the front and the end of each monolith, leaving the end to be less functionalized than the front.

nitrogen mass percentage was too low to be detected by elemental analysis. The middle part revealed a minor degree of functionalization (0.34 mmol g^{-1}), proving that most of the catalyst molecules were grafted within the first part of the monolith. This marked grafting gradient confirms the aforementioned explanation: owing to the hydrophilicity of the aminopropyl group, APTMS cannot form hydrogen bonds with toluene. Accordingly, they favorably stick together in solution, impeding a homogeneous distribution of the silanes in solution, which eventually prohibits homogeneous grafting throughout the whole monolith. Figure 5 schematically depicts the solvent-depending grafting homogeneity.

Additionally, monolith I and one functionalized sample (0.5 equiv of APTMS in ethanol at 50 °C) were studied by diffuse reflectance infrared transform spectroscopy (DRIFTS, Figure 6). Compared to standard IR methods, this technique allows

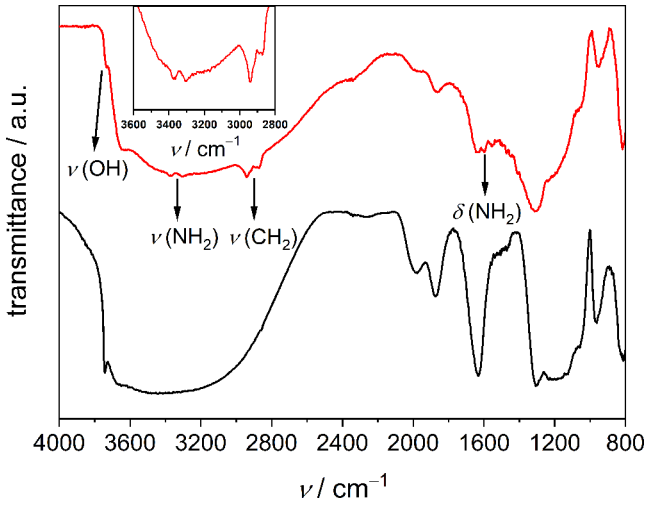

Figure 6. DRIFT spectrum of an unfunctionalized monolith (black) and a monolith after functionalization with APTMS in ethanol (red).

not only the detection of the organic catalyst but also the identification of free silanol groups. The amine group can be detected by its NH stretching modes (3370 and 3300 cm^{-1}), the weak intensity of which results from the underlying broad band of adsorbed water. The deformation modes of the amine group can be assigned to the small peak at 1595 cm^{-1}. Vibrational bands at 2943 and 2871 cm^{-1} refer to the CH stretching modes of the propyl linker. Furthermore, the characteristic vibrational band of the free silanol groups (3745 cm^{-1}) significantly decreases upon grafting.

2.4. Catalytic Test Experiments. The functionalized silica monoliths were used for catalyzing the Knoevenagel condensation under continuous-flow conditions. Distilled benzaldehyde and ethyl cyanoacetate were chosen as reactants and used in the form of solutions in ethanol (c = 0.5 mol L^{-1}) at 22 °C. Additionally, one reaction was conducted at 60 °C to study the influence of temperature. After each flow rate, the monoliths were flushed with 15 mL of ethanol to wash out product residues. A main objective of these experiments was to study the impact of the mesopore size, the grafting density, and the grafting gradient of the catalyst during the functionalization.

First, catalytic experiments were conducted with functionalized monoliths of type I (small mesopores). Monolith I-A was functionalized in toluene at 50 °C, thus exhibiting a large grafting gradient between the front (1.98 mmol g^{-1}) and the end of the monolith (1.08 mmol g^{-1}). Monolith I-B was functionalized in ethanol at 50 °C and offers a homogeneous catalyst loading of about 1.54 mmol g^{-1} throughout the whole monolith. Considering the averaged catalyst loading of reactor I-A (1.57 mmol g^{-1}), both reactors are suitable to test the influence of the grafting gradient on the catalytic performance. As the length of both functionalized monoliths was identical, the amount of catalyst inside both reactors was calculated to be 0.20 mmol. Lowering the flow rate for both reactors steadily increases the yield (Figure 7a), which is expected for such porous materials, as for smaller flow rates a larger number of active sites is accessible for the reactants while passing the monoliths. At the lowest flow rate (0.05 mL min^{-1}), a high yield can be achieved for reactor I-A (92%) as well as for reactor I-B (88%). Hence, although bearing a large grafting gradient, the catalytic performance of reactor I-A coincides well with that of reactor I-B. This result implies that for both types of monoliths all of the mesopores and active sites are equally accessible and that it is the absolute number of catalyst sites on the mesopore surface that determines the yield so that a large grafting gradient does not affect the catalytic performance of the monolith. This finding again confirms the superior pore space of this type of monolithic material, providing unhindered access for both reactants in catalytic reactions.

To study the relevance of the surface concentration of the catalyst, the functionalization temperature in EtOH was lowered to 22 °C to obtain a lower catalyst loading (1.14 mmol g^{-1}, surface concentration 1.7 μmol m^{-2}). Also, in this case (reactor I-C), no grafting gradient was observed. Although containing a slightly lower catalyst amount (0.14 mmol), this monolith (I-C) achieves the highest yield of all

https://dx.doi.org/10.1021/acsomega.0c04857
ACS Omega 2021, 6, 425−437

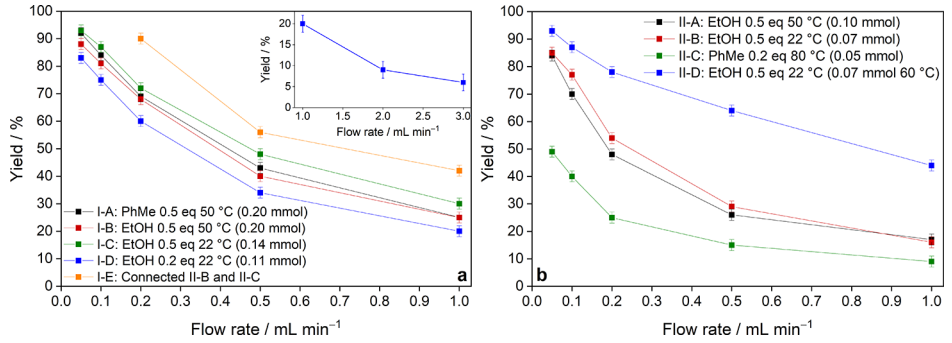

Figure 7. Yield of the continuous-flow catalyzed Knoevenagel condensation with different monoliths based on functionalized monolith I (a) and monolith II (b) depending on the flow rate. The numbers inside the brackets refer to the amount of catalyst inside each reactor. These values were derived from the catalyst loading and the length of the monolith, i.e., the amount of silica inside each reactor.

three reactors. At first glance, an increase in conversion upon reducing the catalyst amount seems counterintuitive. However, the enhanced performance might be caused by the lower density of aminopropyl groups attached to the silica surface (2.4 and 2.3 μmol m^{-2} for monoliths I-A and I-B, respectively). By assuming that nearly all catalyst groups are accessible, reducing the surface coverage of the aminopropyl groups concomitantly results in a higher surface concentration of the remaining silanol groups. These weakly acidic silanol groups can form hydrogen bonds with benzaldehyde, which in turn increases the catalytic performance by cooperative catalysis, as has been demonstrated for amine-functionalized silica materials.[46−50] To lower the catalyst loading even further, one monolith (I-D) was functionalized with 0.2 equiv of APTMS in EtOH at 50 °C. This reactor features an averaged catalyst loading of 0.90 mmol g^{-1} and a surface coverage of 1.4 μmol m^{-2}. Here, the yield is significantly reduced compared to monolith I-C, which exhibits a slightly higher surface coverage and a higher catalyst loading. From this comparison, we infer that the surface coverage of monolith I-C is already low enough and optimal to enable pronounced cooperative catalysis between the catalyst and the surrounding silanol groups. The overall back pressures for the examined flow rates were relatively low owing to the continuous macroporous network of the monoliths. They almost linearly decrease from 7 bar (1.0 mL min^{-1}) down to 1 bar (0.05 mL min^{-1}). In theory, the conversion at high flow rates in such heterogeneous catalytic reactions should decrease because diffusion into the mesopore space is impeded. Hence, the conversion is catalyzed by amino groups on the macropore walls being easily accessible. Thus, the conversion at high flow rates converges to values corresponding to the intrinsic activity of the catalyst. Hence, for one particular monolith (I-D) showing a low back pressure, the flow rates were further increased. Accordingly, the yield decreased from 20% (1.0 mL min^{-1}) to 9% (2.0 mL min^{-1}, 14 bar) and 6% (3.0 mL min^{-1}, 28 bar). For the highest flow rates, monolith I-D thus moves toward a saturation in yield, which can be attributed to the intrinsic activity of the aminopropyl groups, the exact quantification of which can be subjected to further studies.

Additionally, by connecting reactors I-B and I-C, a numbering-up setup was established (I-E), which increases the yield by about 15% (total) for each flow rate compared to the average yield of both reactors alone. Concurrently, the back pressure linearly increases by a factor of 2. Yet, because the back pressures of the monoliths are still low (14 bar at 1.0 mL min^{-1}), connecting such monoliths thus allows for a straightforward increase in the yield without changing other parameters. With this numbering-up setup, it is possible to synthesize 1.1 g (5.4 mmol) of the condensation product per hour for the lowest flow rate (0.2 mL min^{-1}). By increasing the flow rate up to 1.0 mL min^{-1}, about 2.5 g (12.6 mmol) of the product can be obtained per hour, which emphasizes the practical application of the functionalized monoliths.

Analogous catalytic test reactions were carried out with different reactors based on monolith II (Figure 7b) to study the impact of a larger mesopore size. Two of the monoliths were functionalized in ethanol at 50 °C (reactor II-A) and 22 °C (reactor II-B), both possessing homogeneously distributed catalyst loadings of 0.82 mmol g^{-1} (2.7 μmol m^{-2}) and 0.49 mmol g^{-1} (1.6 μmol m^{-2}), respectively. The total amounts of catalyst inside each of these two reactors were calculated to be 0.10 mmol (reactor II-A) and 0.07 mmol (reactor II-B). These lower values for the amount of immobilized catalyst of monolith II are due to the larger mesopore size, which result in a lower surface area and thus lower amounts of grafted catalyst, compared to monolith I. Similar to monolith I, the yield steadily increases upon decreasing the flow rate for both reactors. Notably, reactor II-B displays slightly higher conversion numbers compared to reactor II-A. This is in good agreement with the observation made from reactors I-B and I-C, i.e., the conversion is higher for lower catalyst loadings for both types of monoliths. Hence, by lowering the surface concentration of the aminopropyl groups, the catalytic performance can be, at least to a small extent, enhanced. To address the impact of an inhomogeneous distribution of the catalyst, monolith II was functionalized with 0.2 equiv of APTMS in toluene at 80 °C (reactor II-C). Here, functionalization took place almost completely inside the front of the monolith (1.10 mmol g^{-1}), leaving the end unfunctionalized. The catalytic performance of reactor II-C is significantly lower by about 40−50% (relative) compared to reactors II-A and II-B. Here, both the low amount of catalyst inside the reactor and the high surface concentration (3.7 μmol m^{-2}) impede cooperative catalysis and diminish the catalytic performance compared to reactors II-A and II-B. To study the temperature dependency of the reaction, flow catalysis was performed at 60 °C, using reactor II-B. At such elevated temperatures, the yield can be increased up to 100% (relative) for high flow rates, and at small flow rates, a yield up to 95% can be achieved.

In summary, in comparison to monolith II, the functionalized monoliths of type I (smaller mesopores) still offer a higher catalytic performance, which we attribute to the overall

https://dx.doi.org/10.1021/acsomega.0c04857
ACS Omega 2021, 6, 425−437

higher absolute amount of grafted catalyst inside the reactors. Since the studied microreactors exhibit different catalyst loadings, the catalytic performance of the monoliths was compared regarding their turnover frequencies (TOFs). Based on the concentration of the product $c_{Product}$, the flow rate F, and the amount of catalyst inside the reactor n_{Cat}, the TOF can be calculated by eq 2.

$$\mathrm{TOF} = \frac{n_{Product}}{n_{Cat} t_{Reaction}} = \frac{c_{Product} F}{n_{Cat}} \quad (2)$$

By this approach, we exclude the effect of varying amounts of catalyst inside each reactor. However, one should keep in mind that the uncertainty in the elemental analysis measurements remains constant for each functionalized sample. Thus, the lower the catalyst loading, the higher is the relative error. Since monolith II-C exhibits the lowest amount of catalyst, it was excluded from the TOF calculation as the error bars were too large to perform a meaningful analysis. Even for monolith II-B, the error bars become quite large for higher flow rates. These conditions must be considered when comparing the TOF values of differently functionalized monoliths (Figure 8). By

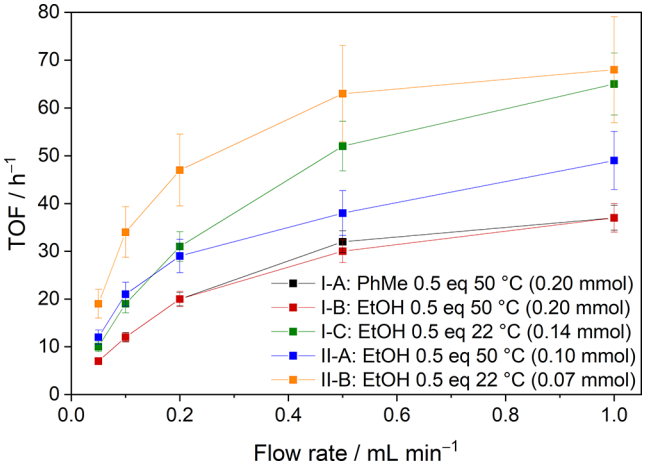

Figure 8. Turnover frequencies of several reactors based on monoliths I (smaller mesopores) and II (larger mesopores).

increasing the flow rate, the TOF values of all reactors steadily increase. Monoliths I-A and I-B, differing only in the spatial homogeneity of the catalyst, feature almost identical TOF values for all flow rates. The TOF values calculated for monolith I-C, which features a lower catalyst loading and a lower surface concentration (1.7 μmol m^{-2}), are significantly larger for every flow rate, which supports the aforementioned considerations that, assuming nearly all aminopropyl groups to be accessible, the reaction rate is enhanced for each catalyst group compared to monoliths I-A and I-B (2.4 and 2.3 μmol m^{-2}, respectively). TOF values calculated for the functionalized reactors based on monolith II (II-A and II-B) behave accordingly: For monolith II-A (2.7 μmol m^{-2}), the corresponding TOF values are significantly lower compared to monolith II-B (1.6 μmol m^{-2}), indicating the proposed cooperative catalysis to be independent of the mesopore size. Notably, TOF values of monoliths II-A and II-B bearing a larger mesopore size are higher compared to the functionalized reactors based on monolith I with smaller mesopores, which we attribute to the enhanced diffusion rate of the reactants inside the larger mesopores.

Although the monolithic reactors offer a good catalytic performance for the Knoevenagel condensation, a comparison with other basic catalysts is needed. For that reason, we conducted the reaction between benzaldehyde and ethyl cyanoacetate in ethanol (both 0.5 mol L^{-1}) with propylamine (5 mol %, equals 0.125 mmol) as a homogeneous organocatalyst (Figure S20). As expected, the yield concurrently increases with reaction time. Since comparing the yield or TOF values between homogeneous and heterogeneous catalysis can be challenging, comparison between both systems was conducted regarding the amount of product that can be synthesized within one hour. Here, the reaction with propylamine produces 412 mg of the product. In comparison, monolith I-C (0.14 mmol) and monolith II-B (0.07 mmol) synthesize 869 mg (0.2 mL min^{-1}) and 652 mg (0.2 mL min^{-1}) of the condensation product, respectively, being more productive than the homogeneous catalyst. Furthermore, the reaction can be performed continuously in flow, while the reaction with propylamine was conducted in a batch reactor. Additionally, we compared the catalytic performance of the functionalized monoliths with the one synthesized by El Kadib et al., featuring comparable porosity parameters (650 m^2 g^{-1}, mesopore diameters within 3−10 nm) to monolith I.[23] The TOF values of monolith I-C (52 h^{-1}) and II-B (63 h^{-1}) for 0.5 mL min^{-1} are lower compared to the TOF values obtained by El Kadib et al. (about 78 h^{-1}). However, these deviations might be assigned to the different reaction conditions. For example, we used ethanol as a solvent for every catalytic reaction, whereas El Kadib et al. conducted their experiments in dimethyl sulfoxide (DMSO). Surface concentration of the catalyst also differed, which was shown to have a strong impact on catalytic performance.

Additionally, product screening was performed with reactor I-C (Table 1) to test the viability of such monoliths for

Table 1. Substrate Scope of the Monolithic Reactor I-C[a]

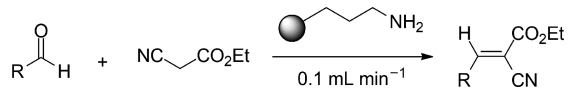

entry	R	c/mol L^{-1}	yield/%	TOF/h^{-1}
1	C_6H_5	0.5	87 ± 2	19 ± 4
2	C_6H_5	0.5	72 ± 2	15 ± 3
3	C_6H_5	0.2	85 ± 2	7 ± 2
4	4-Me-C_6H_4	0.5	75 ± 2	16 ± 3
5	4-Me-C_6H_4	0.2	92 ± 2	8 ± 2
6	4-OMe-C_6H_4	0.5	58 ± 2	12 ± 3
7	4-OMe-C_6H_4	0.2	97 ± 2	8 ± 2
8	4-Cl-C_6H_4	0.5	28 ± 2	6 ± 1
9	4-Cl-C_6H_4	0.2	44 ± 2	4 ± 1
10	4-Ph-C_6H_4	0.1	80 ± 2	3 ± 1

[a]A solvent mixture of ethanol/toluene (1:1, vol %) was used for every reaction expect for entry 1 (pure ethanol).

different aldehydes in the Knoevenagel condensation. Furthermore, different concentrations and solvent compositions were tested to avoid clogging of the reactor with the corresponding product. Consequently, we chose a 1:1 mixture of ethanol and toluene (vol %), providing good solubility of all products. By changing the solvent composition, the yield decreased from 87 to 72% for benzaldehyde, which means that the solvent mixture does exhibit a certain impact on the catalytic performance.[51] Decreasing the concentration of

https://dx.doi.org/10.1021/acsomega.0c04857
ACS Omega 2021, 6, 425−437

benzaldehyde and ethyl cyanoacetate down to 0.2 mol L^{-1} increases the yield to 85% owing to the decreased ratio of the catalyst to the reactants. Because of the smaller concentration of both reactants, the corresponding TOF values decrease similarly. The introduction of a methyl group in the *para*-position only slightly affects the catalytic performance of the reactor (entries 4 and 5). However, reactions with *p*-anisaldehyde (entries 6 and 7) show contradicting behavior. At a concentration of 0.5 mol L^{-1}, the yield drops down to 58%, which is lower compared to both methyl-substituted benzaldehyde and benzaldehyde alone. However, lowering the concentration to 0.2 mol L^{-1} increases the yield to 97% owing to the increased ratio between the catalyst and the reactant molecules. With *p*-chloro-benzaldehyde, the yield significantly decreases for both concentrations. At a concentration of 0.5 mol L^{-1}, a yield of only 28% can be obtained. Decreasing the flow rate to 0.2 mol L^{-1} increases the yield to 44%. Introducing a phenyl group leads to a much bulkier reactant molecule. For this starting material, we had to lower the concentration even further to 0.1 mol L^{-1} to prevent clogging of the reactor, which was noticeable by the strongly increased back pressure. In summary, these experiments show good performance of the reactor for most of the reactants, even for the bulkier phenyl derivative. However, clogging of the reactor has turned out to be a crucial issue in continuous-flow catalysis, which can be prevented by changing the solvent mixture or the reactants' concentrations. However, changing the solvent composition from pure ethanol to ethanol/toluene (entries 1 and 2) can reduce the catalytic performance.

To study the long-term stability of the functionalized monoliths, we tested reactor I-C over a reaction time of 66 h (Figure 9), keeping the flow rate at 0.2 mL min^{-1}.

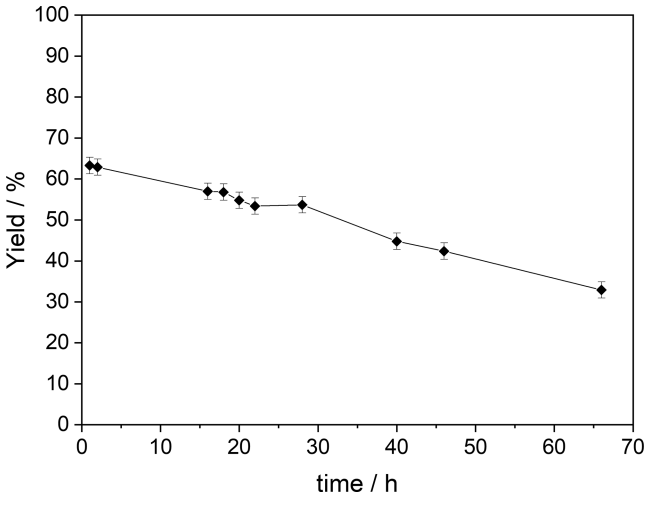

Figure 9. Long-term stability test of reactor I-C. The overall loss in performance was calculated to be about 30%. Reaction conditions: F = 0.2 mL min^{-1}; c(BA) = 0.5 mol L^{-1}; 22 °C.

Starting from 63% yield, the reactor loses almost 10% of its performance every 20 h. After 66 h, a yield of 33% remains. The loss in activity can be attributed to catalyst poisoning with covalently bonded ethyl cyanoacetate.[51,52] Postcatalytic investigation by DRIFT (Figure S19) reveals that the characteristic bands of the free amino group (3370, 3300 cm^{-1}) disappeared. No explicit discussion can be conducted for the band at 1595 cm^{-1} because the intensity of this band was already weak prior to catalysis. At the same time, a distinctive band at 2216 cm^{-1} appears, which can be assigned to the CN stretching mode of ethyl cyanoacetate. Furthermore, the new band at 2983 cm^{-1} might be caused by the CH_2 group of ethyl cyanoacetate. We are aware that this band could also be induced by ethyl cyanoacetate that has not been washed out of the material. However, the reactor was flushed with large quantities of ethanol. Combined with a significant decrease in the free amine groups, we conclude that the catalyst deactivation is mostly due to the covalently attached ethyl cyanoacetate as reported in the literature.[51,52] Then, 1 M HCl and 2.5 M HCl (in ethanol and water, 1:1) were used to cleave the amide bond. However, the amide band was still detectable by DRIFT after the acidic treatment. The acid concentration was not increased to prohibit a removal of the covalently linked APTMS unit by acidic hydrolysis of the siloxane bonds. Furthermore, established amide reduction procedures mostly feature reactive or corrosive chemicals, which would damage our high-performance liquid chromatography (HPLC) pumping system.[53,54]

3. CONCLUSIONS

Meso-macroporous silica monoliths, which are frequently used as the stationary phase in HPLC, were functionalized with a catalytic motif to study fundamental aspects in their use in heterogeneous organocatalysis. (3-Aminopropyl)-trimethoxysilane (APTMS) was immobilized on the pore surface, acting as the catalyst for the Knoevenagel condensation used as the test reaction to study organocatalysis under flow conditions. Since tight housing is inevitable for performing reactions under flow, a suitable polymer cladding procedure was developed based on PEEK. Centimeter-long monoliths with a diameter of 3 mm were encased to ensure crack-free casing along the entire monolith. Various state-of-the-art methods were applied to determine the spatial distribution of the aminopropyl moiety. By combining argon physisorption with elemental analysis and ToF-SIMS measurements, we show that the grafting in ethanol proceeds homogeneously throughout the whole monolith. However, additional ToF-SIMS experiments need to be conducted to study the radial grafting gradient in detail. Grafting in toluene, by contrast, results in pronounced inhomogeneity in the spatial distribution, with the front of each monolith being significantly stronger functionalized than the end. However, no impact of the grafting gradient on the catalytic performance was obtained even under variation of the flow rate if the total amount of catalyst in the reactor was constant. We attribute this tolerance toward spatial inhomogeneity of the catalyst to the generally superior flow properties of these meso-macroporous SiO_2 monoliths, which are based on the favorable three-dimensional (3D) networks of both the mesopore and macropore spaces. Yields between 20 and 90% can be achieved for flow rates of 1.0 and 0.1 mL min, respectively, with small back pressures (7 and 1 bar, respectively), demonstrating the general feasibility and potential of using these monoliths in organocatalysis. Two different sets of monoliths were studied, differing only in the average mesopore dimension (ca. 7 and 16 nm), thus allowing for assessing its impact on the catalytic properties. Using monoliths with larger mesopore dimensions resulted in lower conversion, which we attribute to the overall lower amount of catalyst in the reactor because of the smaller surface area. Interestingly, the TOF values of these functionalized monoliths are higher compared to the ones obtained from the functionalized monoliths with a smaller mesopore size as a

https://dx.doi.org/10.1021/acsomega.0c04857
ACS Omega 2021, 6, 425−437

result of the faster diffusion of the reactant molecules. As a major result, a mean mesopore size of 7 nm provides a promising yield and TOF numbers.

While a material containing only such small mesopores would generate an immense back pressure, these meso-macroporous monoliths are ideal with respect to a balance of high catalyst loading and flow-through properties. Hence, 12.6 mmol (2.5 g) mol of the Knoevenagel product can be synthesized in 1 h using one monolithic column, showing the potential for upscaling, by parallel and serial combination of these monoliths in reactors. Coupling two identical columns in series enhances the yield by 20−30%, which provides a strategy to further increase the yield in a given time. Interestingly, by decreasing the surface concentration of the amine catalyst, the yield and the TOF increased notably. This dependence is probably due to a postulated cooperative catalytic mechanism, involving not only the amino group but also free silanol groups on the surface. Reactant screening showed that the functionalized monoliths are suitable for the synthesis of several condensation products based on different benzaldehyde derivatives. In a catalytic test for 66 h, the monolithic reactors showed promising long-term stability. The yield decreased from 63% down to 33% as indicated by quantitative GCMS. Characterization after the reaction by DRIFT revealed that the loss of activity is due to catalyst poisoning by covalently bonded ethyl cyanoacetate. Although these findings demonstrate the great potential of the functionalized monoliths, additional experiments need to be conducted with respect to the regeneration of the deactivated catalyst. Further studies will be dedicated to the details of this recovery and the long-term use.

4. EXPERIMENTAL SECTION

4.1. Materials. Tetramethyl orthosilicate (TMOS, 99%), dry ethanol (99.5%, extradry, absolute), and dry toluene (99.85%, extradry over a molecular sieve) were purchased from Acros Organics. Poly(ethylene glycol) (PEG, M_n = 10 000) was purchased from Fluka. Ethanol (99.8%) was purchased from Fisher Chemicals. Urea (≥99.5%) and (3-aminopropyl)-trimethoxysilane (APTMS, 97%) were purchased from Sigma-Aldrich. Acetic acid (100%) was purchased from Carl Roth. Methanol (≥99.85%) was purchased from Chemsolute. Benzaldehyde (purified by redistillation, ≥99.5%), ethyl cyanoacetate (≥98%), *p*-chlorobenzaldehyde (97%), *p*-tolualdehyde (97%), and biphenyl-4-carboxaldehyde (99%) were purchased from Aldrich. *p*-Anisaldehyde was purchased from TCI. PEEK tubes (1/4 in. outer diameter × 3.17 mm inner diameter, 50 cm length) were purchased from BGB Analytik. PTFE shrink tubes (shrink rate 4:1) were purchased from AUTEC GmbH. All chemicals were used without further purification.

4.2. Characterization. Argon physisorption measurements were performed in an automated gas adsorption station (Autosorb iQ2, Quantachrome Corporation, Boynton Beach, FL) at 87 K. The silica rods were ground, filled into glass tubes with a cylindrical end, and stabilized at 87 K using a cryostat (CryoSync, Quantachrome Corporation, Boynton Beach, FL). Surface areas were calculated by applying the Brunauer−Emmett−Teller (BET) model to a relative pressure range of p/p_0 = 0.05−0.30. Pore-size distributions were calculated with an NLDFT-Kernel (Ar at 87 K on zeolite/silica, cylindr. pore model, moving point average = 5) applied on the adsorption branch. Bare and functionalized silica monoliths were degassed at 150 and 100 °C, respectively, for 20 h. Both surface area and pore-size distribution calculations were supported by the software ASiQwin, version 4.0. Time-of-flight secondary ion mass spectrometry (ToF-SIMS) measurements were conducted using a ToF.SIMS 5 instrument (IONTOF GmbH, Muenster, Germany), which is equipped with a 25 kV Bi cluster primary-ion gun. For analysis, Bi^{3+} cluster-ions with a primary ion current of 0.167 pA were used. The functionalized silica monoliths were cut into five parts of equal size. Every part was analyzed in spectrometry mode from the middle to the edge of the monolith in three steps. For each step, an area of 150 × 150 μm^2 was analyzed with a resolution of 256 × 256 pixel collecting only positive ions. A dose density limit of 10^{12} ions cm^{-2} was set to calculate the primary ion dose and thus the total ion counts, on which the secondary ion signals (Si^+, CNH_4^+) were normalized. Only a mass resolution of $m/\Delta m$ = 1800 @ m/z = 27.06 u (Si^+) was achieved due to the rough and porous surface of the cut monoliths and the accompanied delay in the flight time. Data evaluation was carried out with the software SurfaceLab 7.0 (IONTOF GmbH). Elemental analysis measurements were performed with a CHN analyzer (Vario MICRO cube, Elementar Analysensysteme GmbH, Langenselbold, Germany). Helium was used as the carrier gas (flow rate: 200 mL min^{-1}). The samples were burned at 1148 °C with 5 mg of O_2 for 90 s. The macropore morphology was examined with a mercury porosimeter (Pascal 140/400 porosimeters, Thermo Fisher Scientific, Rodano, Italy) in a pressure range of 0−400 MPa. Macropore volumes were calculated using Washburn's equation supported by the instruments' software (Sol.I.D). A mercury surface tension of 0.48 N m^{-1} and a contact angle of intruded mercury of 140° were assumed for the calculations. For the reaction control, quantitative gas chromatography (GC) was applied with a gas-phase chromatograph (7890B GC System, Agilent Technologies) and a fused silica GC column (Optima 17 MS) coupled with an mass chromatography (MS) (5977B MSD, Agilent Technologies) using helium as the carrier gas. Calibration curve and quantification were supported by the instrument's software MassHunter Quantitative Analysis, version B.09.00. The morphology of the silica monoliths was examined with a scanning electron microscope (Smart SEM MERLIN, Carl Zeiss, Jena, Germany). IR spectra were measured with an FTIR spectrometer and an exchangeable DRIFT sampling module (Alpha II, Bruker Optik, Ettlingen, Germany). Samples were investigated with 80 scans and a resolution of 4 cm^{-1}. ^1H and ^{13}C spectra were measured with a 400 MHz spectrometer (Bruker Avance III HD, Bruker BioSpin GmbH, Rheinstetten, Germany) at 25 °C. The spectra were calibrated using the deuterated solvent peak ($CDCl_3$).

4.3. Syntheses of the Silica Monoliths. Silica monoliths were synthesized following a modified Nakanishi route.[18,41] A total of 1.21 g of poly(ethylene glycol) (PEG) 10 000 and 0.900 mg of urea were weighed and dissolved in 10 mL of 0.01 M AcOH. The clear solution was stirred and cooled in an ice bath at 0 °C for 20 min. Then, 5.75 g of tetramethyl orthosilicate (TMOS) was added and the solution was stirred at 0 °C for 20 min. The ice bath was displaced by a water bath, and the clear solution was stirred at approximately 22 °C for 10 min. The gelation was performed in stainless steel tubes (inner diameter 3.8 mm, length 15 cm). The steel tubes were placed in a thermostat (Julabo F26, Julabo GmbH, Germany), which was precisely kept at 22 °C. Subsequently, 1.2 mL of the solution was added to each steel tube with a syringe and their

https://dx.doi.org/10.1021/acsomega.0c04857
ACS Omega 2021, 6, 425−437

ends were sealed with a parafilm. After gelation at 22 °C for 18 h, five silica rods were put in a 50 mL centrifuge vessel containing 45 mL of a urea−AcOH solution (9 g of urea in 100 mL of 0.01 M AcOH). For hydrothermal treatment, the centrifuge vessel was tightly closed and placed in an oven. Heating ramps were chosen as follows—monolith I: room temperature to 80 °C within 10 h, no holding time; monolith II: room temperature to 95 °C within 11 h, holding time 10 h. After cooling to room temperature, a solvent exchange was performed using 45 mL of HPLC-methanol for five silica rods. The solvent exchange was repeated every 24 h for 3 days. Finally, the silica rods were calcinated at 330 °C for 15 h (heating ramp: room temperature to 330 °C within 10 h).

4.4. Cladding of the Silica Monoliths with Poly(ether ether ketone) (PEEK). The overall arrangement starting with the gelation in stainless steel tubes for the preparation of silica monoliths with the desired dimensions and ending with a bare continuous-flow reactor is shown in Figure S1. In detail, monolithic silica rods (average length 6−7 cm, average diameter 3 mm) were placed inside cut pieces (slightly shorter than the monolithic rods) of straight PEEK tubes (PEEK tubing (natural): 1/4 in. outer diameter × 3.17 mm inner diameter × 50 cm; thermoformed; straightened with tolerance ±2 cm from the middle; BGB Analytik Vertrieb GmbH, Rheinfelden, Germany), which were surrounded by a heat-shrinkable PTFE tube (1−2 cm longer than the PEEK tubes, TOPCROSS PTFE-4-19,05 natural heat-shrinkable PTFE tube; rate of shrinkage 4:1; AUTEC GmbH, Bad Bellingen, Germany). These pieces were put in a crucible, placed in an oven, and heated up to 362 °C (holding time: 1 h; Nabertherm L 3/11/C450, Nabertherm GmbH, Lilienthal, Germany). However, at this point, it must be realized that a small inaccuracy or inhomogeneity in temperature during this treatment will lead to an inhomogeneous cladding result. When changing the manufacturer of the oven in use or even the model of the oven, the maximal temperature of the procedure must be readjusted. To prevent an inhomogeneous cladding, a precise positioning of the surrounded monoliths is also key for a tight connection between silica and PEEK as the temperature might not be distributed homogeneously throughout the oven (Figure S3). After cooling to about 150 °C, the cladded silica monoliths were taken out of the oven and cooled to room temperature. Finally, both ends of the cladded monolith were smoothly cut and provided with a thread to enable the connection to the continuous-flow setup. It was shown by SEM and mercury porosimetry that there is a tight connection between the monolithic silica and the PEEK tube (Figure S3) as well as that the macroporosity of the monolith is not influenced by the cladding procedure (Figure S4).

4.5. General Procedure for the Functionalization of Cladded Silica Monoliths in Flow. The cladded monoliths were kept in an oven at 80 °C for 24 h. Prior to functionalization, the continuous-flow setup (Figure S2) was flushed with ca. 20 mL of the corresponding solvent. Then, 5 mL of dry toluene or ethanol was added into a heated 15 mL Schlenk tube (kept under argon) before adding APTMS to the solvent. To prevent the solution from leaching out of the monolith, the threads were wrapped in PTFE sealing tape. Afterward, the monolith was flushed with the corresponding solvent and put in a column oven (functionalization at 22 °C was performed without an oven). The Schlenk tube was opened, the intake hose was dipped into the solution, the outtake hose was fixed slightly above the solution, and the Schlenk tube was thoroughly sealed with parafilm (about 60 cm^2). The APTMS solution was pumped through the system with a flow rate of 0.2 mL min^{-1} for 18 h, generating a back pressure of about 1−2 bar. The functionalized monoliths were washed in flow with ca. 25 mL of toluene and ca. 25 mL of ethanol (if functionalized in dry toluene) or with ca. 50 mL of ethanol (if functionalized in dry ethanol) with a flow rate of 0.5 mL min^{-1} (back pressure 3−4 bar). Finally, the washed monoliths were dried at 80 °C for 24 h.

4.6. General Procedure for the Knoevenagel Condensation in Flow. Functionalized and cladded silica monoliths were connected to the HPLC system and flushed with 5 mL of ethanol prior to catalysis. A solution of distilled benzaldehyde (0.5 mol L^{-1}) or other aldehydes and ethyl cyanoacetate (0.5 mol L^{-1}) in ethanol was pumped through the monolith at 22 °C. Aliquots were constantly collected and evaluated by quantitative GC. Before changing the flow rate, the cladded monoliths were flushed with 15 mL of pure ethanol (flow rate 0.5 mL min^{-1}) prior to the next reaction. Yields for each catalytic reaction run were determined by quantitative GC. Therefore, a calibration curve was obtained by measuring an increasing amount of the corresponding product and a continuous amount of *n*-hexadecane (10 μL) as the internal standard. After the reaction solution had passed the reactor several times, aliquots were taken and quantified.

■ ASSOCIATED CONTENT

Supporting Information

The Supporting Information is available free of charge at https://pubs.acs.org/doi/10.1021/acsomega.0c04857.

Physisorption and elemental analysis data of the functionalized silica monoliths, SEM images of the interface of a cladded silica monolith, 3D graphics illustrating the temperature sensitivity of the cladding procedure, additional mercury porosimetry measurements of monolithic silica rods and cladded silica monoliths (PDF)

■ AUTHOR INFORMATION

Corresponding Author

Bernd M. Smarsly − *Institute of Physical Chemistry, Justus Liebig University Giessen, D-35392 Giessen, Germany; Center for Materials Research, D-35392 Giessen, Germany;* orcid.org/0000-0001-8452-2663; Email: Bernd.Smarsly@phys.chemie.uni-giessen.de

Authors

Kevin Turke − *Institute of Physical Chemistry, Justus Liebig University Giessen, D-35392 Giessen, Germany; Center for Materials Research, D-35392 Giessen, Germany*

Rafael Meinusch − *Institute of Physical Chemistry, Justus Liebig University Giessen, D-35392 Giessen, Germany; Center for Materials Research, D-35392 Giessen, Germany*

Pascal Cop − *Institute of Physical Chemistry, Justus Liebig University Giessen, D-35392 Giessen, Germany; Center for Materials Research, D-35392 Giessen, Germany*

Eric Prates da Costa − *Institute of Physical Chemistry, Justus Liebig University Giessen, D-35392 Giessen, Germany; Center for Materials Research, D-35392 Giessen, Germany*

Raoul D. Brand − *Institute of Physical Chemistry, Justus Liebig University Giessen, D-35392 Giessen, Germany; Center for Materials Research, D-35392 Giessen, Germany*

https://dx.doi.org/10.1021/acsomega.0c04857
ACS Omega 2021, 6, 425−437

Anja Henss − *Institute of Physical Chemistry, Justus Liebig University Giessen, D-35392 Giessen, Germany; Center for Materials Research, D-35392 Giessen, Germany;* orcid.org/0000-0001-5009-6512

Peter R. Schreiner − *Institute of Organic Chemistry, Justus Liebig University Giessen, D-35392 Giessen, Germany; Center for Materials Research, D-35392 Giessen, Germany;* orcid.org/0000-0002-3608-5515

Complete contact information is available at: https://pubs.acs.org/10.1021/acsomega.0c04857

Author Contributions

The manuscript was written through contributions of all authors. All authors have given approval to the final version of the manuscript.

Notes

The authors declare no competing financial interest.

■ ACKNOWLEDGMENTS

This project was supported by the Center for Materials Research (LaMa) of the Justus-Liebig-University Giessen, Germany. We cordially thank Elisabeth Kalden from Goethe-Universität Frankfurt am Main for the numerous elemental analysis measurements.

■ REFERENCES

(1) Porta, R.; Benaglia, M.; Chiroli, V.; Coccia, F.; Puglisi, A. Stereoselective Diels-Alder Reactions Promoted under Continuous-Flow Conditions by Silica-Supported Chiral Organocatalysts. *Isr. J. Chem.* **2014**, *54*, 381−394.

(2) Chiroli, V.; Benaglia, M.; Cozzi, F.; Puglisi, A.; Annunziata, R.; Celentano, G. Continuous-flow Stereoselective Organocatalyzed Diels-Alder Reactions in a Chiral Catalytic "Homemade" HPLC Column. *Org. Lett.* **2013**, *15*, 3590−3593.

(3) Akwi, F. M.; Watts, P. Continuous flow chemistry: where are we now? Recent applications, challenges and limitations. *Chem. Commun.* **2018**, *54*, 13894−13928.

(4) Losch, P.; Kolb, J. F.; Astafan, A.; Daou, T. J.; Pinard, L.; Pale, P.; Louis, B. Eco-compatible zeolite-catalysed continuous halogenation of aromatics. *Green Chem.* **2016**, *18*, 4714−4724.

(5) Jin, R.; Zheng, D.; Liu, R.; Liu, G. Silica-Supported Molecular Catalysts for Tandem Reactions. *ChemCatChem* **2018**, *10*, 1739−1752.

(6) Chong, A. S. M.; Zhao, X. S.; Kustedjo, A. T.; Qiao, S. Z. Functionalization of large-pore mesoporous silicas with organosilanes by direct synthesis. *Microporous Mesoporous Mater.* **2004**, *72*, 33−42.

(7) Díaz, U.; Brunel, D.; Corma, A. Catalysis using multifunctional organosiliceous hybrid materials. *Chem. Soc. Rev.* **2013**, *42*, 4083.

(8) Liang, J.; Liang, Z.; Zou, R.; Zhao, Y. Heterogeneous Catalysis in Zeolites, Mesoporous Silica, and Metal−Organic Frameworks. *Adv. Mater.* **2017**, *29*, No. 1701139.

(9) Ferré, M.; Pleixats, R.; Wong Chi Man, M.; Cattoën, X. Recyclable organocatalysts based on hybrid silicas. *Green Chem.* **2016**, *18*, 881−922.

(10) Fődi, T.; Kupai, J.; Túrós, G.; Németh, T.; Rojik, E.; Riethmüller, E.; Balogh, G. T.; Huszthy, P. Application of Flow Chemistry to Macrocyclization of Crown Ethers. *J. Flow Chem.* **2016**, *6*, 297−301.

(11) Schulze, J. S.; Migenda, J.; Becker, M.; Schuler, S. M. M.; Wende, R. C.; Schreiner, P. R.; Smarsly, B. M. TEMPO-functionalized mesoporous silica particles as heterogeneous oxidation catalysts in flow. *J. Mater. Chem. A* **2020**, *8*, 4107−4117.

(12) Ishitani, H.; Furiya, Y.; Kobayashi, S. Continuous-flow synthesis using a column reactor packed with heterogeneous catalysts: A convenient production of nitroolefins by using amino-functionalized silicagel. *Bioorg. Med. Chem.* **2017**, *25*, 6229−6232.

(13) Kasaplar, P.; Rodríguez-Escrich, C.; Pericàs, M. A. Continuous Flow, Highly Enantioselective Michael Additions Catalyzed by a PS-supported Squaramide. *Org. Lett.* **2013**, *15*, 3498−3501.

(14) Tsubogo, T.; Oyamada, H.; Kobayashi, S. Multistep continuous-flow synthesis of (*R*)- and (*S*)-rolipram using heterogeneous catalysts. *Nature* **2015**, *520*, 329−332.

(15) Enke, D.; Gläser, R.; Tallarek, U. Sol-Gel and Porous Glass-Based Silica Monoliths with Hierarchical Pore Structure for Solid-Liquid Catalysis. *Chem. Ing. Tech.* **2016**, *88*, 1561−1585.

(16) Galarneau, A.; Abid, Z.; Said, B.; Didi, Y.; Szymanska, K.; Jarzębski, A.; Tancret, F.; Hamaizi, H.; Bengueddach, A.; Di Renzo, F.; Fajula, F. Synthesis and Textural Characterization of Mesoporous and Meso-/Macroporous Silica Monoliths Obtained by Spinodal Decomposition. *Inorganics* **2016**, *4*, No. 9.

(17) Berdys, M.; Koreniuk, A.; Maresz, K.; Pudło, W.; Jarzębski, A. B.; Mrowiec-białon, J. Fabrication and performance of monolithic continuous-flow silica microreactors. *Chem. Eng. J.* **2015**, *282*, 137−141.

(18) Nakanishi, K.; Soga, N. Phase Separation in Gelling Silica−Organic Polymer Solution: Systems Containing Poly(sodium styrenesulfonate). *J. Am. Ceram. Soc.* **1991**, *74*, 2518−2530.

(19) Alotaibi, M.; Manayil, J. C.; Greenway, G. M.; Haswell, S. J.; Kelly, S. M.; Lee, A. F.; Wilson, K.; Kyriakou, G. Lipase immobilised on silica monoliths as continuous-flow microreactors for triglyceride transesterification. *React. Chem. Eng.* **2018**, *3*, 68−74.

(20) Hou, C.; Ghéczy, N.; Messmer, D.; Szymańska, K.; Adamcik, J.; Mezzenga, R.; Jarzębski, A. B.; Walde, P. Stable Immobilization of Enzymes in a Macro- and Mesoporous Silica Monolith. *ACS Omega* **2019**, *4*, 7795−7806.

(21) Nagaki, A.; Hirose, K.; Tonomura, O.; Taniguchi, S.; Taga, T.; Hasebe, S.; Ishizuka, N.; Yoshida, J. I. Design of a Numbering-up System of Monolithic Microreactors and Its Application to Synthesis of a Key Intermediate of Valsartan. *Org. Process Res. Dev.* **2016**, *20*, 687−691.

(22) Sachse, A.; Galarneau, A.; Fajula, F.; Di Renzo, F.; Creux, P.; Coq, B. Functional silica monoliths with hierarchical uniform porosity as continuous flow catalytic reactors. *Microporous Mesoporous Mater.* **2011**, *140*, 58−68.

(23) El Kadib, A.; Chimenton, R.; Sachse, A.; Fajula, F.; Galarneau, A.; Coq, B. Functionalized Inorganic Monolithic Microreactors for High Productivity in Fine Chemicals Catalytic Synthesis. *Angew. Chem., Int. Ed.* **2009**, *48*, 4969−4972.

(24) Haas, C. P.; Müllner, T.; Kohns, R.; Enke, D.; Tallarek, U. High-performance monoliths in heterogeneous catalysis with single-phase liquid flow. *React. Chem. Eng.* **2017**, *2*, 498−511.

(25) Brühwiler, D. Postsynthetic functionalization of mesoporous silica. *Nanoscale* **2010**, *2*, 887−892.

(26) Weng, Z.; Yu, T.; Zaera, F. Synthesis of Solid Catalysts with Spatially Resolved Acidic and Basic Molecular Functionalities. *ACS Catal.* **2018**, *8*, 2870−2879.

(27) Minakuchi, H.; Nakanishi, K.; Soga, N.; Ishizuka, N.; Tanaka, N. Octadecylsilylated Porous Silica Rods as Separation Media for Reversed-Phase Liquid Chromatography. *Anal. Chem.* **1996**, *68*, 3498−3501.

(28) Morisato, K.; Miyazaki, S.; Ohira, M.; Furuno, M.; Nyudo, M.; Terashima, H.; Nakanishi, K. Semi-micro-monolithic columns using macroporous silica rods with improved performance. *J. Chromatogr. A* **2009**, *1216*, 7384−7387.

(29) Kohns, R.; Haas, C. P.; Höltzel, A.; Splith, C.; Enke, D.; Tallarek, U. Hierarchical silica monoliths with submicron macropores as continuous-flow microreactors for reaction kinetic and mechanistic studies in heterogeneous catalysis. *React. Chem. Eng.* **2018**, *3*, 353−364.

(30) Liang, C.; Dai, S.; Guiochon, G. Use of gel-casting to prepare HPLC monolithic silica columns with uniform mesopores and tunable macrochannels. *Chem. Commun.* **2002**, *2*, 2680−2681.

(31) Ritter, H.; Brühwiler, D. Accessibility of Amino Groups in Postsynthetically Modified Mesoporous Silica. *J. Phys. Chem. C* **2009**, *113*, 10667−10674.

(32) Zhu, M.; Lerum, M. Z.; Chen, W. How to Prepare Reproducible, Homogeneous, and Hydrolytically Stable Aminosilane-Derived Layers on Silica. *Langmuir* **2012**, *28*, 416−423.
(33) Suzuki, T. M.; Yamamoto, M.; Fukumoto, K.; Akimoto, Y.; Yano, K. Investigation of pore-size effects on base catalysis using amino-functionalized monodispersed mesoporous silica spheres as a model catalyst. *J. Catal.* **2007**, *251*, 249−257.
(34) Galarneau, A.; Sachse, A.; Said, B.; Pelisson, C.-H.; Boscaro, P.; Brun, N.; Courtheoux, L.; Olivi-Tran, N.; Coasne, B.; Fajula, F. Hierarchical porous silica monoliths: A novel class of microreactors for process intensification in catalysis and adsorption. *C. R. Chim.* **2016**, *19*, 231−247.
(35) Sharma, K. K.; Anan, A.; Buckley, R. P.; Ouellette, W.; Asefa, T. Toward Efficient Nanoporous Catalysts: Controlling Site-Isolation and Concentration of Grafted Catalytic Sites on Nanoporous Materials with Solvents and Colorimetric Elucidation of Their Site-Isolation. *J. Am. Chem. Soc.* **2008**, *130*, 218−228.
(36) Sharma, K. K.; Asefa, T. Efficient Bifunctional Nanocatalysts by Simple Postgrafting of Spatially Isolated Catalytic Groups on Mesoporous Materials. *Angew. Chem., Int. Ed.* **2007**, *46*, 2879−2882.
(37) Sharma, K. K.; Buckley, R. P.; Asefa, T. Optimizing Acid−Base Bifunctional Mesoporous Catalysts for the Henry Reaction: Effects of the Surface Density and Site Isolation of Functional Groups. *Langmuir* **2008**, *24*, 14306−14320.
(38) Chamieh, J.; Zimmermann, Y.; Boos, S.; Hagège, A. Short communication A simple cladding process to apply monolithic silica rods in high performance liquid chromatography. *J. Chromatogr. A* **2010**, *1217*, 7172−7176.
(39) Knoevenagel, E. Condensation von Malonsaeure mit aromatischen Aldehyden durch Ammoniak und Amine. *Ber. Dtsch. Chem. Ges.* **1898**, *31*, 2596−2619.
(40) List, B. Emil Knoevenagel and the Roots of Aminocatalysis. *Angew. Chem., Int. Ed.* **2010**, *49*, 1730−1734.
(41) Meinusch, R.; Ellinghaus, R.; Hormann, K.; Tallarek, U.; Smarsly, B. M. On the underestimated impact of the gelation temperature on macro- and mesoporosity in monolithic silica. *Phys. Chem. Chem. Phys.* **2017**, *19*, 14821−14834.
(42) Cychosz, K. A.; Guillet-Nicolas, R.; García-Martínez, J.; Thommes, M. Recent advances in the textural characterization of hierarchically structured nanoporous materials. *Chem. Soc. Rev.* **2017**, *46*, 389−414.
(43) Thommes, M.; Cychosz, K. A. Physical adsorption characterization of nanoporous materials: Progress and challenges. *Adsorption* **2014**, *20*, 233−250.
(44) Thommes, M.; Kaneko, K.; Neimark, A. V.; Olivier, J. P.; Rodriguez-Reinoso, F.; Rouquerol, J.; Sing, K. S. W. Physisorption of gases, with special reference to the evaluation of surface area and pore size distribution. *Pure Appl. Chem.* **2015**, *87*, 1051−1069.
(45) Zhuravlev, L. T. The surface chemistry of amorphous silica. Zhuravlev model. *Colloids Surf., A* **2000**, *173*, 1−38.
(46) Hruby, S. L.; Shanks, B. H. Acid-base cooperativity in condensation reactions with functionalized mesoporous silica catalysts. *J. Catal.* **2009**, *263*, 181−188.
(47) Collier, V. E.; Ellebracht, N. C.; Lindy, G. I.; Moschetta, E. G.; Jones, C. W. Kinetic and Mechanistic Examination of Acid-Base Bifunctional Aminosilica Catalysts in Aldol and Nitroaldol Condensations. *ACS Catal.* **2016**, *6*, 460−468.
(48) Corma, A.; Iborra, S.; Rodríguez, I.; Sánchez, F. Immobilized Proton Sponge on Inorganic Carriers: The Synergic Effect of the Support on Catalytic Activity. *J. Catal.* **2002**, *211*, 208−215.
(49) Motokura, K.; Tada, M.; Iwasawa, Y. Heterogeneous Organic Base-Catalyzed Reactions Enhanced by Acid Supports. *J. Am. Chem. Soc.* **2007**, *129*, 9540−9541.
(50) Kane, A.; Deshpande, N.; Brunelli, N. A. Impact of surface loading on catalytic activity of regular and low micropore SBA-15 in the Knoevenagel condensation. *AIChE J.* **2019**, *65*, No. e16791.
(51) Macquarrie, D. J.; Clark, J. H.; Lambert, A.; Mdoe, J. E. G.; Priest, A. Catalysis of the Knoevenagel reaction by γ-aminopropylsilica. *React. Funct. Polym.* **1997**, *35*, 153−158.
(52) Wirz, R.; Ferri, D.; Baiker, A. ATR-IR Spectroscopy of Pendant NH_2 Groups on Silica Involved in the Knoevenagel Condensation. *Langmuir* **2006**, *22*, 3698−3706.
(53) Behloul, C.; Guijarro, D.; Yus, M. Deacylation of Esters, Thioesters and Amides by a Naphthalene-Catalysed Lithiation. *Synthesis* **2006**, No. 2, 309−314.
(54) O' Donovan, D. H.; De Fusco, C.; Spring, D. R. The Reductive Cleavage of Picolinic Amides. *Tetrahedron Lett.* **2016**, *57*, 2962−2964.

https://dx.doi.org/10.1021/acsomega.0c04857
ACS Omega 2021, 6, 425−437